NDT Plus (2011) 4: 313–317
doi: 10.1093/ndtplus/sfr076
Advance Access publication 25 July 2011

Case Report

NDT PLUS
Nephrology Dialysis Transplantation

Unusual cases of hydronephrosis with retroperitoneal fibrosis: mystery revealed

Rupesh Raina[1], James F. Simon[1], Chad R. Marion[3], Arrossi Valeria[2], Sankar D. Navaneethan[1], Gustavo A. Heresi[2], Jorge A. Guzman[4], Edgard Wehbe[1] and Joseph V. Nally[1]

[1]Department of Nephrology and Hypertension, Glickman Urological and Kidney Institute, Cleveland Clinic, Cleveland, OH, USA, [2]Department of Anatomic Pathology, Pathology Laboratory and Medicine Institute, Cleveland Clinic, Cleveland, OH, USA, [3]Department of Internal Medicine, Medicine Institute, Cleveland Clinic, Cleveland, OH, USA and [4]Department of Pulmonary and Critical Care Medicine, Respiratory Institute, Cleveland Clinic, Cleveland, OH, USA

Correspondence and offprint requests to: Rupesh Raina; E-mail: rainar@ccf.org

Keywords: Erdheim–Chester disease; histiocytosis; renal failure; retroperitoneal fibrosis; urinary tract obstruction

Introduction

Retroperitoneal fibrosis encompasses a range of diseases characterized by the presence of a fibro-inflammatory tissue, which usually surrounds the abdominal aorta, iliac arteries and extends into the retroperitoneum to envelop neighboring structures such as the ureters.

We present two cases with multisystem disease involving retroperitoneal fibrosis, renal failure, pulmonary infiltrates and skeletal abnormalities. The unifying diagnosis of Erdheim–Chester disease (ECD) is a non-Langerhans cell histiocytosis (NLH) characterized by bilateral metaphyseal sclerosis of long bones, retroperitoneal fibrosis and multiple organ dysfunction due to the infiltrative process.

Case 1

A 34-year-old Caucasian female presented with shortness of breath, progressive weight gain and leg pain. Two years earlier, she was seen in the emergency department for left flank pain. She was diagnosed with recurrent pancreatitis and underwent a cholecystectomy. Her course was complicated by the development of a pancreatic pseudocyst, splenic vein thrombosis with massive splenomegaly, multiple left peri-renal fluid collections and retroperitoneal fibrosis, all of which were attributed to the pancreatitis. She required left ureteral stent placement for hydronephrosis that resulted from ureteral obstruction by the retroperitoneal fibrosis.

Postoperatively, she developed acute kidney injury with a peak serum creatinine of 300.5 μmol/L (baseline 3 months prior was 79 μmol/L) that responded to intravenous fluids. A urological consultation recommended a Technetium-99m -Mag-3 scan which revealed left and right differential renal function of 15 and 85%, respectively.

At presentation, she was alert but with labored breathing on 50% vent mask. Jugular veins were distended, crackles were present in all lung fields and bilateral lower extremity edema was noted. On admission, sodium was 144 mmol/dL, potassium 3.5 mmol/L, serum bicarbonate 34 mmol/dL, blood urea nitrogen 4.4 mmol/L and creatinine was 200 μmol/L.

Chest x-ray revealed increased interstitial infiltrates and bilateral pleural effusions. Ejection fraction was normal on echocardiography. Right heart catherization revealed elevated right-sided pressures consistent with pulmonary hypertension. Urine examination showed red blood cells and granular casts but no proteinuria. Fractional excretion of sodium was $<1\%$. On renal ultrasonography, the right kidney was 12 cm and the left kidney was 10 cm with cortical thinning without hydronephrosis.

She failed to diurese with intravenous furosemide and developed hypoxic and hypercarbic respiratory failure requiring intubation. Nephrology was consulted for consideration of urgent dialysis for volume removal but they did not feel that volume overload alone explained her clinical presentation. Renal Doppler findings were as follows: right renal artery origin peak systolic velocity, 413 cm/s; end diastolic volume, 207 cm/s with right renal artery to aortic ratio, 6.1. The diagnosis of right renal artery stenosis, 80-99% severity was made. It was postulated that renal artery stenosis involving a solitary functioning kidney was causing the pulmonary edema.

Slow continuous ultrafiltration was initiated with transition to intermittent hemodialysis. A computerized tomography (CT) revealed multilobar pneumonia and extensive retroperitoneal fibrosis involving the right renal artery leading to compression of the renal arteries. Because of the atypical nature of her presentation and the concern for malignancy, she underwent a left-sided open lung biopsy which demonstrated foamy histiocytic infiltrate in left upper lobe (Figure 1A and B) staining negative for S-100, positive

CD68 staining and negative CD1a staining (Figure 1Ca and Cb). Her respiratory status improved and she was extubated. She complained of worsening bilateral lower extremity pain unresponsive to narcotics. X-rays of her legs revealed abnormal sclerosis in the distal two-thirds of the tibia and fibula sparing the epiphyses, irregular cortical lucencies, cortical thickening and narrowing of the medullary canals (Figure 2A and B).

Based upon the radiographic and pathological findings, the diagnosis of ECD was made. Treatment with intravenous methyl prednisone was initiated. Within 1 week, she had improvement in renal function such that dialysis could be discontinued. The ureteral stent was left in place due to concerns about ureteral compression by the retroperitoneal fibrosis. The pulmonary infiltrates also improved, but the bone pain did not resolve by the time of discharge. Despite her impressive initial response to steroids, her disease did not completely remit. She was later treated with steroids, imatinib mesylate and interferon alpha. Despite this, she passed away 8 months later from respiratory failure.

Case 2

A 66-year-old Caucasian male presented as a hospital transfer with increased shortness of breath and acute kidney injury. Six months prior to admission, he was admitted to a local hospital with pneumonia; he had a newly diagnosed non-ischemic cardiomyopathy with an ejection fraction of 25%. His subsequent course included two episodes of acute decompensated heart failure, a pulmonary embolism and a diagnosis of diabetes insipidus.

During his last admission, he developed acute kidney injury with bilateral hydronephrosis for which ureteral stents and eventually nephrostomy tubes were placed. Despite this, his renal function continued to decline and he was initiated on intermittent hemodialysis. CT revealed pulmonary infiltrates, pleural effusions, cardiomegaly, mediastinal lymphadenopathy, perinephric effusions and perinephric stranding.

At presentation upon transfer, he appeared chronically ill but in no acute distress. Physical examination was notable for lack of elevation of jugular venous pressure or crackles on lung exam. The abdomen was tympanitic, distended and diffusely tender with voluntary guarding but without fluid wave; 2+ bilateral lower extremity pitting edema was present.

Renal ultrasonography revealed mild right hydronephrosis, left upper pole caliectasis and a small right perinephric fluid collection. Echocardiogram revealed an improved ejection fraction of 45%. He developed a persistent sense of dyspnea despite the lack of overt hypoxia. The discordance between his infiltrates/dyspnea and lack of hypoxia or abnormal lung findings on exam led to the discussion of whether the process was pulmonary edema or an infiltrative process. Ultrafiltration was performed for two sequential

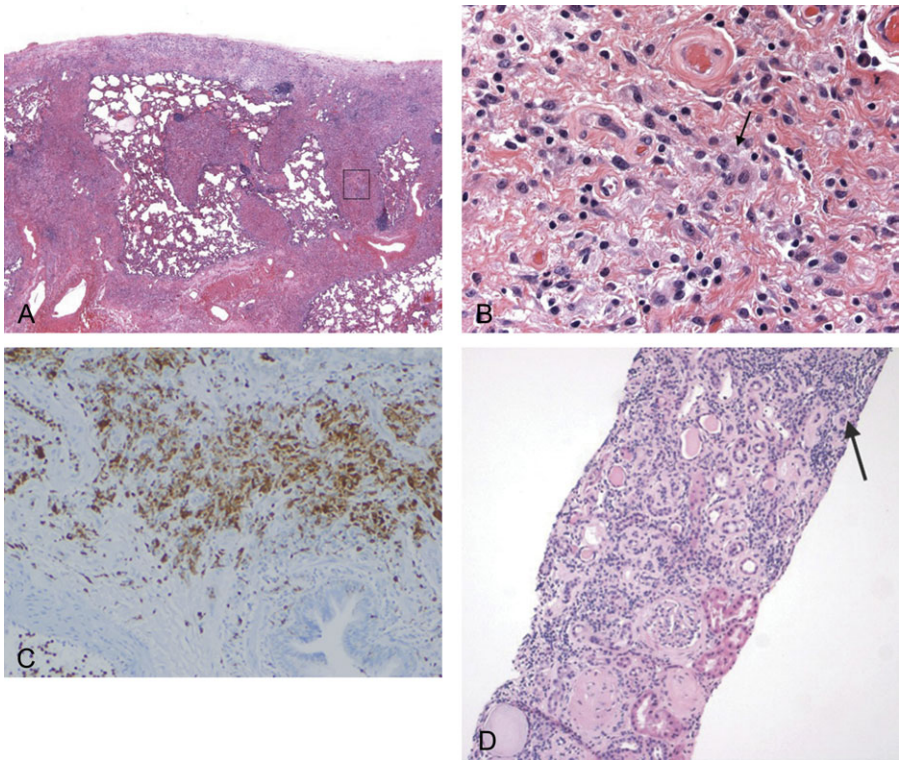

Fig. 1. (**A**) Magnification (×25) of lung tissue demonstrating histiocytic infiltration of the subpleural and intralobar septa. (**B**) Magnification (×40) of lung tissue from the boxed area in Figure 1A. This demonstrates histiocytic proliferation with fibrosis in a subpleural and bronchovascular bundle distribution indicated by >. (**C**) Magnification (×20) of lung tissue histiocyte staining for CD68 (brown area) in Figure Ca and but CD1a negative in Figure Cb. (**D**) Magnification (×10) of renal tissue demonstrating interstitial fibrosis and chronic inflammation marked by > that stained negative for CD1a (not shown).

days without improvement in his symptoms or the infiltrates seen on repeat CT, strongly suggesting against pulmonary edema as the cause of his presentation. A nuclear medicine whole body positron emission tomography with radiolabeled [^{18}F]-2-fluoro-deoxy-D-glucose (PET-FDG) scan was performed due to the seemingly unrelated multi-organ involvement to try to obtain a unifying diagnosis. This showed increased FDG uptake in the lungs, pleura, adrenal glands, kidneys, mediastinal and retroperitoneal lymph nodes and along the entire vasculature (Figure 3A and B). CT of the brain showed bilateral retro-orbital infiltrative soft tissue masses. When the report of his repeat chest CT returned, the diagnosis of ECD was suggested based upon the persistent nature of the atypical infiltrates. Subsequent radiography of lower extremities showed symmetric cortical thickening and sclerosis of the tibia and fibula. Kidney biopsy revealed mixed inflammatory infiltrate and staining for S-100, Langerin and CD1a revealed non-Langerhans histiocytes (Figure 1D).

Once the unifying diagnosis of ECD was made, he was treated with pulse IV solumedrol followed by oral prednisone. He had rapid improvement in pulmonary symptoms and kidney function improved such that hemodialysis could be discontinued. The ureteral stents were left in place. Four months after initiation of therapy, he developed recurrence of fatigue and new bone pain when the prednisone dose was tapered to 20 mg daily. Second agent cladribine (a purine analogue toxic to monocytes) was added with improvement in respiratory and pulmonary symptoms but he ultimately died with sepsis after 10 months.

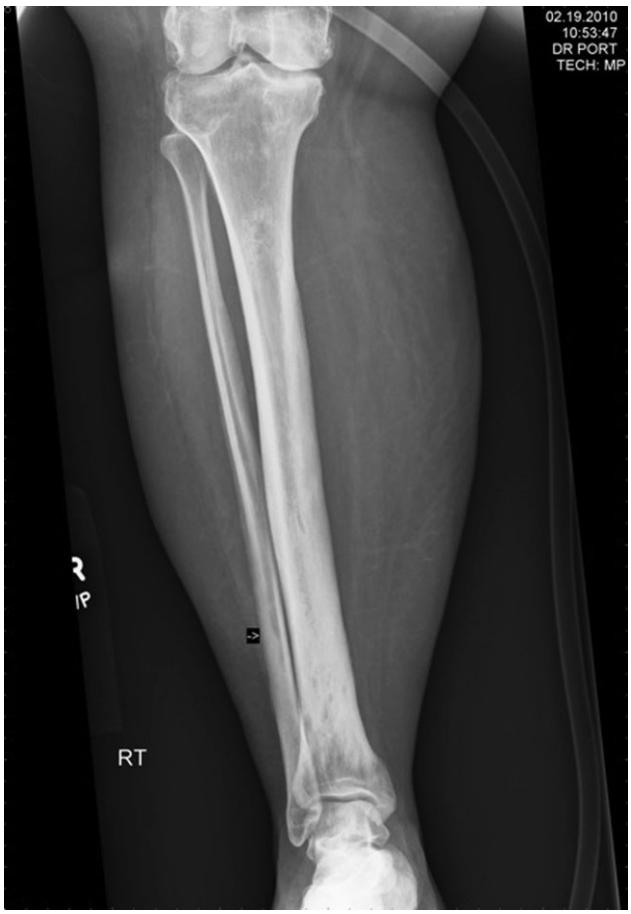

Fig. 2. XR tibia fibula AP/LAT. The tibias show abnormal sclerosis in the distal two-thirds with sparing of the epiphyses. There is some irregular lucency. Cortical thickening is present with resultant narrowing of the medullary canals indicated by >. Similar findings are present in each fibula predominantly distally as well as both femurs.

Discussion

Our two patients exemplify the classic presentation of an unusual, life-threatening multisystem disease, which may be responsive to therapy if correctly identified. Both patients had retroperitoneal fibrosis, pulmonary infiltrates, long bone abnormalities, hydronephrosis and eventually renal failure requiring hemodialysis. In both cases, biopsies revealed foamy histiocytes, lymphocytes and scattered giant cells infiltrating affected organs, while plain film x-rays showed symmetric cortical thickening and sclerosis of tibia and fibula. The diagnosis of (Letterer) ECD was suggested by radiographic findings in both cases, bone findings in the first case and atypical pulmonary infiltrates in the second.

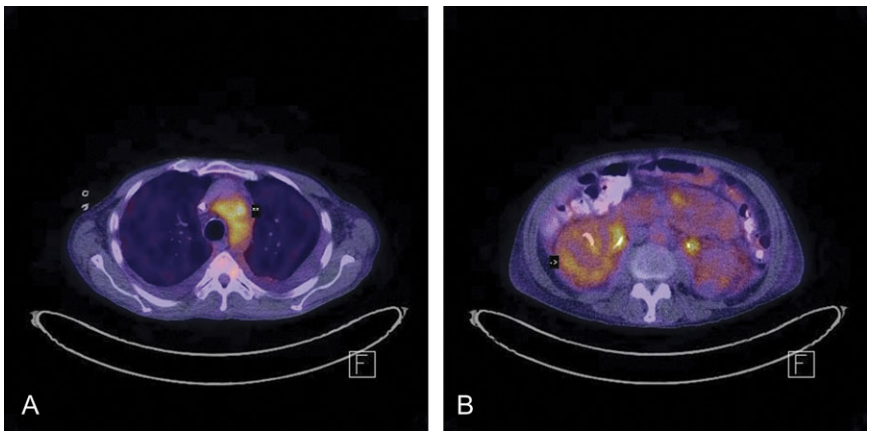

Fig. 3. Whole body FDG-PET demonstrates diffuse increased vascular markings in the lung, pleural, adrenals and kidneys consistent with inflammatory or infectious process. (**A**) **Illustrates a representative area of aortic FDG uptake. (**B**) >Indicates a representative area of renal FDG uptake.

Histologic confirmation of the diagnosis was made by biopsy of the involved organs. Tables 1 and 2 summarize the clinical manifestations, histopathology and immunochemical staining of this disorder. Following the diagnosis of ECD, steroids were initiated and transient improvement was noted with recovery of renal function in both cases.

The prevalence of ECD compared to other forms of histiocytosis is unknown but ~327 cases have been described in the literature [1]. The mean age at the time of diagnosis was 53 years with a slight male predominance [2]. This disease manifests with infiltration of multiple organ sites by foamy histiocytes, lymphocytes and scattered giant cells with extensive fibrosis [3].

Classically, ECD presents with symmetric long bone pain caused by histiocyte infiltration. Other clinical manifestations depend on the organ involvement but commonly include respiratory infiltrates, retroperitoneal fibrosis and renal failure (Tables 1 and 2) [2–4]. Our cases illustrate the classic features of ECD despite subtle variations in presentation. The cortical sclerosis seen in ECD is so nearly pathognomic for this disease that the diagnosis was suggested by the radiologist in the first case. While the patient in Case 2 did not complain of the bone pain, the classic radiographic bone findings were still present.

The infiltrative process involving the kidneys can be diagnosed by renal biopsy, as was seen in Case 2. Accumulation of foamy histiocytes without Birbeck granules is seen in a background of chronic interstitial inflammation and fibrosis. Tissue does not stain for S-100 protein or leukocyte antigen CD1, in contrast to histiocytosis X [3–5]. Biopsy of other involved organs will demonstrate a similar histiocyte-staining pattern, as with the lung biopsy in Case 1.

The pathogenesis of renal failure in ECD is due to a combination of histiocytic infiltration of the renal parenchyma and vasculature and urinary outflow obstruction from the retroperitoneal fibrosis [6–8]. Contrast-enhanced CT may show infiltration of the peri-renal fat and the perirenal fascia, leading to a picture termed ‘hairy kidneys’ [7, 8]. The retroperitoneal fibrosis in ECD typically compresses the middle and distal ureters [7–9], which is in contrast with other causes of retroperitoneal fibrosis, which preferentially affects pelvic ureters.

In a review of all published reports of ECD (323 papers and 357 cases), Sanchez found renal involvement was reported in only 11% of cases. Renal involvement consisted of an obstructive uropathy due to retroperitoneal fibrosis (79%) or renal histiocytic infiltration (21%). Renal involvement had a slight male predominance (63% of cases). While all ages could be affected, most patients were in the fifth or sixth decades. Dion *et al.* [6] reported a series of 60 patients with ECD, of which 18 (30%) developed acute kidney injury. Seven of these (39%) presented with hydronephrosis, while 6 (33%) presented with bilateral enlarged kidneys and minimal hydronephrosis. The degree of renal infiltration in these case series is likely underestimated as not all patients underwent a renal biopsy.

PET-CT imaging in ECD has yet to be described in the literature. The diffuse vascular inflammation found on the PET-CT in Case 2 suggests that this disease is not limited

Table 1. Classification of histiocytic disorders

Class I: Langerhans cell histiocytosis
Eosinophilic granuloma, Hand-Schuller-Christian disease, Letterer-Siwe disease (Abt Letterer Siwe disease)
Class II: NLH
Hemophagocytic lymphohistiocytosis (familial erythrophagocytic lymphohistiocytosis), virus-associated hemophagocytic syndrome, sinus histiocytosis with massive lymphadenopathy (Rosai–Dorfman disease), ECD, xanthogranuloma, xanthoma disseminatium, reticulohistiocytoma, juvenile xanthogranulomatosis
Class III: malignant histiocytic disorders
Acute monocytic leukemia, malignant histiocytosis, histiocytic lymphoma

(Adapted from 1, 2).

Table 2. Langerhans versus non-Langerhans cell histiocytoses

Variables	Langerhans cell	Non-Langerhans cell
Age	Children and juveniles	
Histopathology	Bone-marrow derived antigen presenting cells not of monocyte-macrophage lineage	Infiltration of multiple organ sites by foamy histiocytes, lymphocytes and scattered Touton giant cells with extensive fibrosis
Immunohistochemical staining	CD1a+, S-100+, CD68−	CD1a−, S-100 essentially negative, CD68+
Clinical manifestations	Irregular lytic lesions in the medulla, usually with endosteal erosion usually sparing hands and feet	Symmetric, sclerotic lesions of long bones
	Proptosis, rare vision loss	Dyspnea and respiratory failure due to interstitial lung disease
	Destruction of ossicles and deafness and mastoid pain	Hydronephrosis and renal failure secondary to retroperitoneal xanthogranulomatosis
	Seborrhea-like skin papules on back, palms, and sole	Diabetes insipidus
	Hepatic dysfunction	Extra-axial masses (dural nodules)
	Cough, tachypnea, pneumothorax with pulmonary involvement	Retro-orbital masses with visual disturbances
	Hyperprolactinemia and hypogonadism from hypothalamic infiltration	Ataxia secondary to cerebellar involvement
		Pericardial infiltration may lead to pericardial effusion

(Adapted from 1–3).

solely to the organs that are clinically involved but also represents a more disseminated process involving the vasculature and multiple other organs.

Treatment for this disease remains controversial. Due to the rarity of the disease, no randomized controlled therapeutic trials have been conducted. The standard treatment recommendation is a trial of steroid therapy [3]. Case reports have evaluated cladribine (a purine analogue toxic to monocytes) and interferon alpha (which results in terminal differentiation of histiocytes and dendritic cells) mainly in patients with exophthalmos, bone involvement or bilateral hydronephrosis [10]. Recently, imatinib mesylate (a tyrosine kinase inhibitor which selectively inhibits bcr-abl, KIT and platelet-derived growth factor) was reported to be partially effective for multisystem disease. A single case of treatment of refractory ECD with double autologous hematopoietic stem cell transplantation has been reported [9].

ECD is associated with a relatively grave prognosis. In a review of 59 patients, Veyssier-Belot reported deaths related to the ECD in 59% of the cases, with an average survival of 32 months. The most common causes of death were respiratory and heart failure. The authors suggested that patients with ECD have a poorer prognosis than those with NLH [2]. In general, the prognosis is dismal as most patients died within 5 years of diagnosis [1].

We treated our patients with high-dose steroids alone. Both showed dramatic improvement in their respiratory status and renal failure. Both patients remained stable at follow-up 4 months after initiation of steroid therapy; however, neither patient had their disease successfully suppressed long term with steroid therapy. Our cases are typical of patients with ECD in that they had several organ systems effected in seemingly unrelated fashion without a good reason. It was not until the classic bone abnormalities were seen of x-ray or the typical histiocytic infiltration was documented on biopsy that the diagnosis was made. Interestingly, radiologists were the first to suggest the diagnosis in both cases.

In summary, although ECD is a rare disorder, it is necessary to consider as a possible cause of renal failure, especially in the differential diagnosis of cases with urinary tract obstruction, retroperitoneal fibrosis with pulmonary infiltrates or bone disease. Diagnosis of this rare condition is difficult, but if made, may be lifesaving.

Funding. This publication was made possible by grant number RR024990 (S.D.N.) from the National Center for Research Resources (NCRR), a component of the National Institutes of Health (NIH), and NIH Roadmap for Medical Research. Its contents are solely the responsibility of the authors and do not necessarily represent the official view of NCRR or NIH. Information on NCRR is available at http://www.ncrr.nih.gov/. Information on Re-engineering the Clinical Research Enterprise can be obtained from http://nihroadmap.nih.gov/clinicalresearch/overview.

Conflict of interest statement. None declared.

References

1. Sanchez JE, Mora C, Macia M *et al.* Erdheim-Chester disease as cause of end-stage renal failure: a case report and review of the literature. *Int Urol Nephrol* 2010; 42: 1107–1112
2. Veyssier-Belot C, Cacoub P, Caparros-Lefebvre D *et al.* Erdheim-Chester disease: clinical and radiologic characteristics of 59 cases. *Medicine (Baltimore)* 1996; 75: 157–169
3. Kenn W, Stabler A, Zachoval R *et al.* Erdheim-Chester disease: a case report and literature overview. *Eur Radiol* 1999; 9: 153–158
4. Fink MG, Levinson DJ, Brown NL *et al.* Erdheim-Chester disease: case report with autopsy findings. *Arch Pathol Lab Med* 1991; 115: 619–623
5. Egan AJ, Boardman LA, Tazelaar HD *et al.* Erdheim-Chester disease: clinical, radiologic, and histopathology findings in five patients with interstitial lung disease. *Am J Surg Pathol* 1999; 23: 17–2
6. Dion E, Graef C, Haroche J *et al.* Imaging of toracoabdominal involvement in Erdheim Chester disease. *Am J Roentgenol* 2004; 183: 1253–1260
7. Brian J, Douglas P. Erdheim-Chester disease of the retorperitoneum. *Am J Roentgenol* 2001; 176: 1130–1131
8. Wimpissinger TF, Schernthaner G, Feichtinger H *et al.* Compression of kidneys in Erdheim-Chester disease of retroperitoneum: open surgical approach. *Urology* 2005; 65: 798
9. Verdalles U, Goicoechea M, García de Vinuesa S *et al.* Erdheim–Chester disease: a rare cause of renal failure. *Nephrol Dial Transplant* 2007; 22: 1776–1777
10. Haroche J, Amoura Z, Trad SG *et al.* Variability in the efficacy of interferon-alpha in Erdheim-Chester. *Arthritis Rheum* 2006; 54: 3330–3336

Received for publication: 1.4.11; Accepted in revised form: 27.5.11